Cell Metabolism
Article

The Oscillating miRNA 959-964 Cluster Impacts *Drosophila* Feeding Time and Other Circadian Outputs

Sadanand Vodala,[1] Stefan Pescatore,[1] Joseph Rodriguez,[1] Marita Buescher,[2] Ya-Wen Chen,[2] Ruifen Weng,[2] Stephen M. Cohen,[2,3] and Michael Rosbash[1,*]
[1]Howard Hughes Medical Institute, National Center for Behavioral Genomics, Department of Biology, Brandeis University, Waltham, MA 02454, USA
[2]Institute of Molecular and Cell Biology, 61 Biopolis Drive, Singapore 138673, Singapore
[3]Department of Biological Sciences, National University of Singapore, Singapore 117543, Singapore
*Correspondence: rosbash@brandeis.edu
http://dx.doi.org/10.1016/j.cmet.2012.10.002

SUMMARY

We sequenced *Drosophila* head RNA to identify a small set of miRNAs that undergo robust circadian cycling. We concentrated on a cluster of six miRNAs, mir-959-964, all of which peak at about ZT12 or lights off. The cluster pri-miRNA is transcribed under bona fide circadian transcriptional control, and all six mature miRNAs have short half-lives, a requirement for cycling. A viable Gal4 knockin strain localizes prominent cluster miRNA expression to the adult head fat body. Analysis of cluster knockout and overexpression strains indicates that innate immunity, metabolism, and feeding behavior are under cluster miRNA regulation. Manipulation of food intake also affects the levels and timing of cluster miRNA transcription with no more than minor effects on the core circadian oscillator. These observations indicate a feedback circuit between feeding time and cluster miRNA expression function as well as a surprising role of posttranscriptional regulation in the circadian control of these phenotypes.

INTRODUCTION

Many organisms have circadian pacemakers that control their physiology and behavior (Golombek and Rosenstein, 2010). These clocks are entrained by external cues like light and temperature (*Zeitgebers*) and maintain a rhythm of about 24 hr or precisely 24 hr under entrainment conditions. Transcriptional feedback loops play an important role in timekeeping. Positive factors like CLOCK (CLK) and CYCLE (CYC) in *D. melanogaster* or CLK and BMAL1 in mammals lead to the transcription of negative regulators like PERIOD (PER) and TIMELESS (TIM), or PER and CRYPTOCHROME (CRY), respectively. The negative regulators gain entry to the nucleus, collaborate with kinases and chromatin factors, and then repress CLK-CYC- and CLK-BMAL1-mediated transcription. The negative regulators decay, and circadian transcription begins anew (Allada and Chung, 2010).

In contrast to the abundant information on the transcriptional regulation of circadian rhythms, less is known about posttranscriptional regulation, for example, the circadian regulation of mRNA turnover (So and Rosbash, 1997; Woo et al., 2010; Woo et al., 2009). However, recent work from several labs has addressed the contribution of miRNAs to circadian rhythmicity (see below).

miRNAs are endogenous, ~22 nucleotide small noncoding RNAs. They function predominantly by binding either in the 3′UTR or open reading frame (ORF) of a target mRNA and affect translational regulation and/or lead to decreases in target mRNA levels (Guo et al., 2010; Karginov et al., 2010). miRNAs are generated by cleavage reactions (Ghildiyal and Zamore, 2009; Miyoshi et al., 2010). Drosha processes the pri-miRNA primary transcript within the nucleus to a single hairpin-containing pre-miRNA transcript. It is exported to the cytoplasm where it is processed by Dicer and loaded into an effector RNP complex (RNA-induced silencing complex, RISC). The miRNA-containing RISC complex then interacts with target mRNAs.

In mice, Cheng et al. (2007) highlighted the role of two brain-specific miRNAs, miR-219 and miR-132, and their contribution to circadian clock modulation. miR-132 has also been shown to target a number of genes involved in chromatin remodeling and translational control, which then modulate Period gene activity (Alvarez-Saavedra et al., 2011). The liver-specific miR-122 has been shown to play a role in the rhythmic expression of the circadian deadenylase nocturnin in mice (Kojima et al., 2010). Rhythmic expression of chicken mir-26a has been shown to modulate the protein expression of photoreceptor L-type voltage-gated calcium channel alpha1C subunit (Shi et al., 2009).

Two *Drosophila* miRNAs, dme-miR-263a and dme-miR-263b, have been reported to exhibit circadian oscillations and are predicted to target *clk* and or *cwo* (Yang et al., 2008). A more recent study from our laboratory demonstrated that *clk* translation is modulated by the developmental miRNA *bantam*, thus affecting the core circadian clock (Kadener et al., 2009).

To further investigate the role of miRNAs in the *Drosophila* circadian system, we used the Illumina platform to sequence 18–29 nt RNA and compared six circadian time points. Although most miRNAs showed little or no significant oscillations, there were a few exceptions. We focused on a cluster of six miRNAs, all of which showed high amplitude cycling. The miRNA

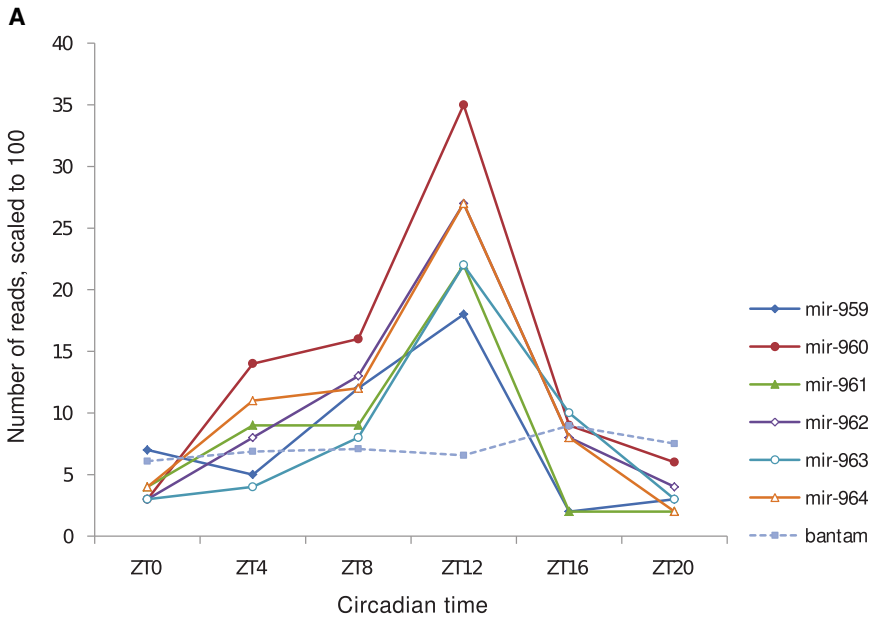

Figure 1. Identification of Cycling miRNAs via Illumina Deep Sequencing

Small RNA libraries for Illumina deep sequencing platform were prepared from fly head RNA across six different circadian time points. The number of reads for each miRNA was normalized to total number of reads from each time point and plotted across six circadian time points.

(A) The abundance of a cluster of six miRNAs (miR-959, miR-960, miR-961, miR-962, miR-963, and miR-964) and the developmental regulator miRNA *bantam* is plotted across circadian time. Except *bantam*, all six candidates show high amplitude of cycling. The actual number of reads for *bantam* was 10,000 fold more across all six time points than the plotted values.

(B) The sequences of a cluster of six cycling miRNAs (miR-959 to miR-964). The underlined sequence is the seed region which is different for each member.

B

miR-959 - uugucaucgggguauuaugaa
miR-960 - ugaguauuccagauugcauagc
miR-961 - uuugaucaccaguaacugagau
miR-962 - auaagguagagaaauugaugcuguc
miR-963 - acaagguaaauaucagguuguuuc
miR-964 - uuagaauaggggagcuuaacuu

oscillations are under circadian regulation, as they disappear in three arrhythmic strains: *clkAR*, *clkJRK*, and *per01*. The cluster pri-miRNA also shows comparable circadian cycling and becomes arrhythmic in the *per01* strain, suggesting that circadian transcriptional regulation makes a major contribution to the miRNA oscillations. Starvation as well as restricted feeding indicate that pri-miRNA circadian transcription is under nutritional/feeding control and disassociates it from the core clock. Identification of target mRNAs using knockout (KO) as well as overexpression strains shows significant overlap and implicates genes involved in various physiological functions including metabolism, oxidative stress, reproductive behavior, peptidase/proteases, and immune function. Consistent with some of these functions, the normal regulation of feeding behavior, immune function, and possibly stress responses is compromised in the KO and/or overexpression strains. Our findings suggest that the cluster miRNAs are synthesized in response to nutritional signals acquired by feeding and then serve to regulate a number of physiological and behavioral responses. These include feeding itself, which suggests a posttranscriptional feedback loop involved in the timing of feeding.

RESULTS

The miRNA 959–964 Cluster Is under Circadian Control

To search for miRNAs under circadian regulation, we sequenced small RNAs around the clock. To this end, small RNA libraries (RNA size 19–29 nucleotides long) were prepared from *Canton S* fly heads collected at six different circadian time points during a light-dark cycle: ZT0 (*Zeitgeber* time 0), ZT4, ZT8, ZT12, ZT16, and ZT20. Sequencing was via the Illumina deep sequencing platform, and an average of 3.1 million reads per time point mapped to unique locations on the genome. Individual miRNA reads were normalized to the total number of miRNA reads from each time point. To search for cycling miRNAs, the number of individual reads was plotted across the six time points, and the graphs were visually inspected.

Although most of the 196 known miRNAs did not show any obvious circadian oscillations across the 24 hr cycle, the six miRNAs 959–964 correspond to a previously characterized miRNA cluster and showed a similar phase and robust amplitude; they are probably encoded on a single transcription unit (Figure 1A; see below). The six miRNAs are encoded within two adjacent introns of CG31646 (miR-959–962 within one, and miR-963-964 within the other; see Figure S1 online). Transcription is antisense to CG31646, which has no known regulatory influence on the cluster. Note that the miRNAs 959–964 have different seed sequences (Figure 1B). We focused the rest of this work on these miRNAs and refer to them subsequently as the "cluster miRNAs."

miRNA RT-PCR (Chen et al., 2005) confirmed the sequencing data; namely, the levels of the cluster miRNAs undergo robust cycling with similar amplitude (Figure 2A). Moreover, all miRNA levels peak at about ZT12 (Figure 2A), consistent with the peak time determined by Illumina sequencing (Figure 1A for 960). *Bantam* miRNA was assayed in parallel and was noncycling or much less obviously cycling across all six time points (Figure 2A), consistent with the sequencing data (Figure 1A). Importantly, there is no cluster miRNA cycling in two classical *clk* arrhythmic mutant strains, *clkAR* and *clkJRK*. This indicates that miRNA cycling requires a functional clock, i.e., an external light:dark

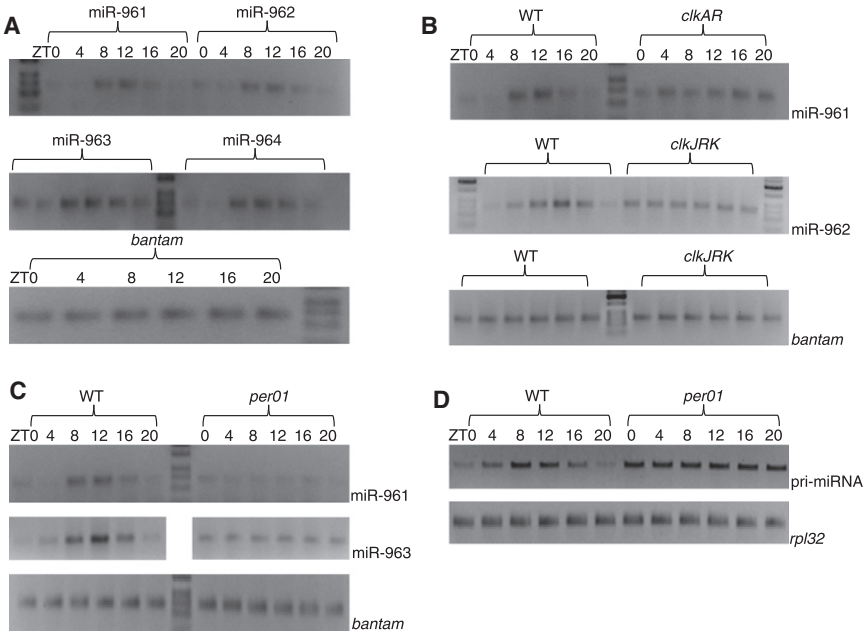

Figure 2. A Cluster of Six miRNAs Show Cycling and Are under Circadian Clock Control

Total RNA was extracted from fly heads across six circadian time points and used for miRNA RT-PCR using miRNA-specific primers (see the Experimental Procedures). A discrete band around 70 base pairs is the PCR product for a mature miRNA.

(A) Shown here are four representatives from a cluster of six miRNAs—miR-961, miR-962, miR-963, and miR-964—all of which show robust oscillation with a peak around ZT12. The developmental regulator miRNA *bantam* was used as a control for RT-PCR which did not show any oscillation.

(B) To investigate the role of circadian clock, we assayed cycling and levels in two *clk* mutants *clkAR* and *clkJRK* by RT-PCR. The levels of the mature miRNA in both *clkAR* and *clkJRK* were comparable to wild-type (WT) and did not show any oscillation in the two mutants. As controls, we assayed the levels of bantam in WT and *clkJRK* flies and did not observe any significant changes.

(C) Wild-type and *per01* flies were entrained in LD conditions, and fly head RNA was extracted from six circadian time points. The levels of the mature miRNA were assayed using miRNA RT-PCR, and as shown earlier the mature miRNA levels showed robust oscillation in WT flies but were arrhythmic in *per01* mutant flies. The overall levels of the mature miRNA also showed ~2- to 3-fold decrease in the *per01* mutant flies. As a control, we assayed the levels of *bantam* miRNA which showed similar levels in WT and *per01* flies.

(D) The levels of the pri-miRNA were analyzed across circadian time in WT and *per01*. The levels of the pri-miRNA showed robust oscillation in the WT flies but did not oscillate in *per01* mutant flies. In fact, pri-miRNA levels were high across all six time points.

cycle is insufficient to drive cluster miRNA cycling (Figure 2B). There was also no apparent cycling in a third arrhythmic mutant strain (Figure 2C).

To assay pri-miRNA expression, we used primers between miRNA 962 and 963, between the two introns of CG31646 (Figure 2D). In WT strains, cluster pri-miRNA undergoes a robust circadian oscillation with a phase and amplitude very similar to those of the miRNAs. This suggests that circadian transcriptional regulation is a critical feature of miRNA cycling dynamics. Cycling was notably absent in the arrhythmic *per01* strain, suggesting that the clock regulates cluster circadian transcription (Figure 2D). Because the pri-miRNA level is quite high whereas miRNA levels are quite low in *per01* flies, the clock may also affect posttranscriptional processing of the cluster miRNAs (see the Discussion).

Generation and Characterization of Cluster Knockin and Knockout Mutants

A cluster miRNA mutant missing miR-959-962 was generated using homologous recombination-based ends-out gene targeting (Gong and Golic, 2003). Because these four miRNAs are located within a single intron of the CG31646 locus (Figure S1), a targeting vector was prepared with homology regions contained within that intron. The DNA was amplified and cloned into the targeting vector pW25-Gal4-attB2 (Weng et al., 2009). It allows introduction of *Gal4* and the *mini-white* marker in place of the miRNA following homologous recombination (Figure 3A). The reporter genes in this knockin strain are flanked by *loxP* sites to permit subsequent excision of the *Gal4* and *mini-white* reporter cassette. Flies carrying the targeted allele were crossed to flies carrying a heat-shock promoter-driven *Cre* recombinase transgene, and progeny lacking the *mini-white* marker were selected on the basis of eye color. Homozygous KO lines were established and the absence of the miRNA cluster DNA confirmed by PCR. The KO lines contain a single *loxP* site in place of the four miRNAs within the CG31646 intron (Figure 3A).

The miR-959-962 KO mutant was homozygous viable and fertile. Quantitative real-time PCR analysis using RNA isolated from the central nervous systems of homozygous miR-959-962 mutant third-instar larvae showed no detectable miR-962 miRNA. In contrast, the levels of miR-963 were not reduced (data not shown). Similar results were observed by assaying all six miRNAs with miRNA-specific RT-PCR using adult head RNA from the KO strain as a template: miR-963-964 were detected, whereas miR-959-962 were not (Figure 3B).

The *Gal4* gene present in the knockin strain was used to assess head tissue expression of the cluster. The strain was crossed to UAS-mCD8GFP and "brains" stained for GFP expression at two time points, ZT12 and ZT0. The brains were not well cleaned, so that adjacent head tissue could be assayed. Staining was prominent in the pericerebral fat body, which was assessed by comparison to the well-characterized *Lsp2-Gal4* driver. Although this tissue is probably not the sole site of cluster expression (see below), the pattern suggests that the fat body is a major site of cluster miRNA expression. Moreover, staining was much stronger at ZT12 than at ZT0, consistent with the cluster miRNA analyses. This suggests that *Gal4* is under the circadian transcriptional regulation that normally governs cluster expression.

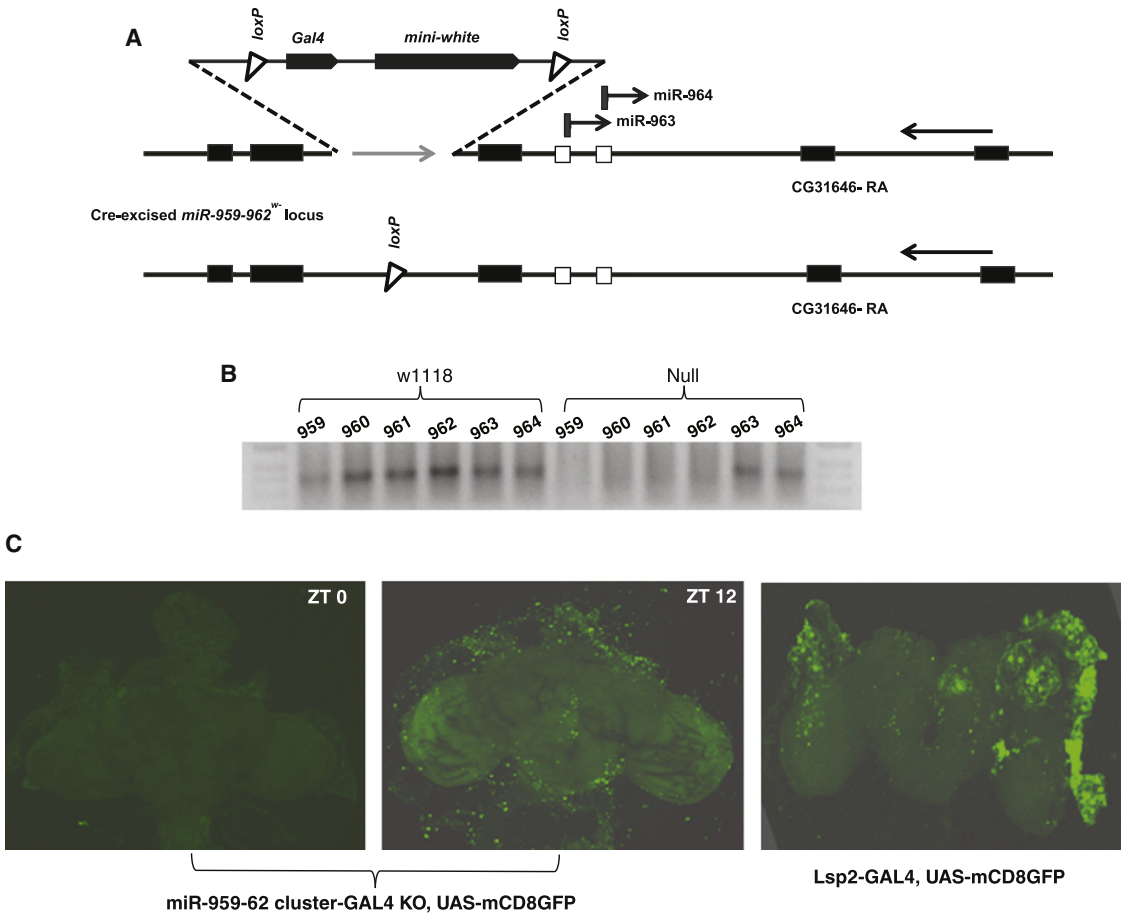

Figure 3. Generation of the Cluster Knockout and Characterization of Cluster Expression

The miR-959-962 KO mutant was generated using homologous recombination-based ends-out gene targeting (Gong and Golic, 2003). Upstream and downstream homology arms flanking miR-959-962 cluster were amplified and cloned into a targeting vector.

(A) The targeting vector *pW25-Gal4-attB2* would allow *Gal4* and *mini-white* gene knockin at the targeted locus. Therefore *miR-959-962 cluster-Gal4 KO* is a *Gal4* knockin mutant and can be used as a *Gal4* driver to report the cluster expression pattern. *miR-959-962 cluster KO^{w-}* was generated from *Gal4* and *mini-white* knock-in mutant by using *Cre/loxP* recombination to excise both *Gal4* and *mini-white* genes.

(B) Total RNA was extracted from *w118* and the KO flies, and all cluster members were assayed by miRNA RT-PCR. The miR 959-962 KO flies lacked the expression of the miR-959, miR-960, miR-961, and miR-962, whereas the expression of miR-963 and miR-964 was unaffected.

(C) The *Gal4* knockin mutant was crossed to UAS-mCD8GFP line, and intact brains were dissected to check for expression of the reporter gene. The brains were not cleaned thoroughly to assay the pericerebral tissue. Gal4 under the control of the cluster miRNA promoter shows circadian oscillation with higher levels at ZT12 as manifested by the expression of the reporter gene GFP. Moreover, GFP showed strong localization in the pericerebral fat body. Lsp2-Gal4 was used as a control for pericerebral fat body localization.

Possible Functions of the Cluster miRNAs from Affected mRNAs

To address possible functions of the cluster miRNAs, the KO strain, as well as a cluster overexpression strain, was compared with companion WT strains. The overexpression strain was a stable line containing the broad circadian driver *tim-gal4* and a UAS-cluster genomic DNA transgene. This was favored over a fat body driver because of the possibility of non-fat body expression. Indeed, cluster miRNA levels in RNA from purified LNvs (Nagoshi et al., 2010; Kula-Eversole et al., 2010) were similar to those from heads relative to bantam miRNA (data not shown). Overexpression of the six cluster miRNAs at all circadian times was apparent by RT-PCR of head RNA (Figure S2).

We first assayed circadian behavior in the two strains relative to companion WT strains. The period of the KO strain period is short by about 30 min, whereas the period of the overexpression strain is long by more than an hour (Figure S3). Although this period alteration could reflect effects from the fat body, we favor the interpretation that it derives from circadian neuron expression.

mRNA changes in the KO and cluster overexpression strains relative to their WT counterparts were then assayed on Affymetrix expression arrays. The strategy was based on the observation that miRNAs often cause a decrease in the steady-state levels of their target mRNAs (Guo et al., 2010; Lim et al., 2005). To accommodate the possibility that important mRNA changes only appear at certain circadian times, RNA was assayed from heads collected at two different times, ZT4 and ZT16, and a criterion of 1.5-fold was used to identify mRNAs altered in the overexpression and the KO strains.

Table 1. DAVID GO Analysis Enriched Categories for Immune Function and Metabolism

GO TERM	Number of Genes	Benjamini Value
ZT4 – Null		
Immune response	15	$3.3\ E^{-04}$
Oxidation reduction	26	$6.4\ E^{-03}$
Antimicrobial humoral response	8	$2.1\ E^{-02}$
ZT4 – Overexpression		
Oxidation reduction	68	$2.3\ E^{-07}$
Innate immune response	17	$5.2\ E^{-03}$
Peptidase M13, neprilysin	10	$1.0\ E^{-03}$
Enzyme inhibitor activity	19	$3.2\ E^{-03}$
ZT16 – Null		
Oxidation reduction	86	$3.7\ E^{-11}$
Proteolysis	96	$4.3\ E^{-11}$
Postmating behavior	15	$6.8\ E^{-11}$
Behavior	18	$2.6\ E^{-08}$
Peptidase activity	93	$5.0\ E^{-08}$
ZT16 – Overexpression		
Oxidation reduction	108	$8.5\ E^{-16}$
Extracellular region	87	$6.5\ E^{-12}$
Proteolysis	104	$1.4\ E^{-09}$
Postmating behavior	14	$8.2\ E^{-09}$
Peptidase activity	106	$3.7\ E^{-08}$

Total RNA was extracted from wild-type, null, and cluster overexpression flies at ZT4 and ZT16 time points, and microarrays were performed as described by the supplier (Affymetrix). We looked for mRNAs whose levels went up in the null and down in the overexpression flies by at least 1.5-fold, and Gene Ontology (GO) analysis was performed using DAVID.

Many individual mRNAs were altered in the two strains and some in opposite directions, i.e., up in the KO strain and down in the overexpression strain; this makes them candidate direct target mRNAs (Table S1). Moreover, many putative target 3′UTRs have predicted miRNA seed-complementary sequences, and some of these 3′UTRs are cluster miRNA targets in S2 cell reporter gene assays (Figure S4).

To address possible biological functions, we searched for GO terms that were enriched in the putative target mRNAs. The most consistent categories were metabolism (oxidation reduction) and immune function, both of which appeared in the overexpression as well as the KO strain data (Table 1). However, "immunity" was only apparent in the ZT4 data. Proteolysis or related terms were enriched in the ZT16 data (Table 1); they might also reflect immune function, as many immunity-relevant proteins are cleaved for activation. Indeed, Ance-4 is related to metalloproteases, and Drosomycin (Drs) is an innate immunity peptide; both mRNAs are cluster targets by S2 cell criteria (Figure S4). Both of these functions, metabolism/feeding and innate immunity, are consistent with the relatively prominent fat body expression of the cluster miRNAs (Figure 3C). It is, however, possible that the proteolysis term is unrelated to immune function and that the difference between the ZT4 and ZT16 terms just reflects circadian regulation (see below).

The Cluster miRNAs Modulate Immune Function and Feeding

To assay immune function, flies were infected with an attenuated strain of *Pseudomonas aeruginosa* (PA14 *plcs*) at the reported peak survival time of ZT17 and assayed for colony-forming units per fly (cfu/fly) 24 hr postinfection (Lee and Edery, 2008). Cluster miRNA overexpression caused substantially higher bacterial titers (~7-fold) compared to the control strains, whereas the KO strain had lower titers compared to its control strain (Figure 4A). The data suggest that the miRNAs inhibit immune function against this specific pathogen and/or change the peak survival time.

To test the second possibility, the KO and its companion WT strain were infected at different ZTs (zeitgeber time; circadian time, but in an LD cycle). The survival curve of the WT strain at 48 hr postinfection was indistinguishable from that originally reported by Lee and Edery, 2008 (Figures 4B and 4C). In contrast, the cluster KO strain had a dramatically shifted curve. The fact that there is still a survival curve in this strain suggests that there are other circadian modulators of immune function and/or that the light cycle has a prominent impact. In either case, the data indicate that the cycling miRNAs contributes to the temporal regulation of immune function, at least against *Pseudomonas aeruginosa* (Figures 4B and 4C and see the Discussion).

To address food/metabolism, the strain overexpressing the cluster and the KO strain were assayed compared to control strains in a typical starvation-feeding paradigm: flies were assayed for food intake in the 15 min after transfer to normal food following 16 hr of starvation. Flies overexpressing the cluster showed a dramatic increase in food consumption after starvation compared to control flies, whereas KO flies ate less than control flies. This was especially apparent in females (Figure 4D).

To gain insight into this feeding behavior phenotype, we watched and videotaped flies after the 16 hr of starvation, immediately after transfer from starvation vials to food vials (Movie S1). A phenotype was particularly apparent in KO female flies, which were hyperactive compared to control flies. It was as if they could not "focus" on feeding. One interpretation is that the miRNAs suppress a foraging response, which is normally induced by 16 hr of starvation. The role of the miRNAs in suppression of foraging could lead to an apparently paradoxical feeding response in a vial: in the KO strain, enhanced foraging would lead to reduced food consumption. In the wild, however, low cluster miRNAs levels in the late night/early morning would not only lead to increased foraging but also to increased feeding.

Feeding Regulates Cluster miRNA Expression

This interpretation suggests that the cluster miRNA expression itself might be regulated by food availability; i.e., successful feeding regulates the timing of cluster miRNA expression, which then suppresses the timing of foraging and food intake as well as the extent and timing of immune function and metabolism. To test this prediction, we first assayed miRNA expression under the conditions used for the feeding assays; i.e., flies were starved and then assayed for cluster miRNA expression and cycling.

Under these conditions, cluster miRNAs remain at the low levels characteristic of late night or very early morning,

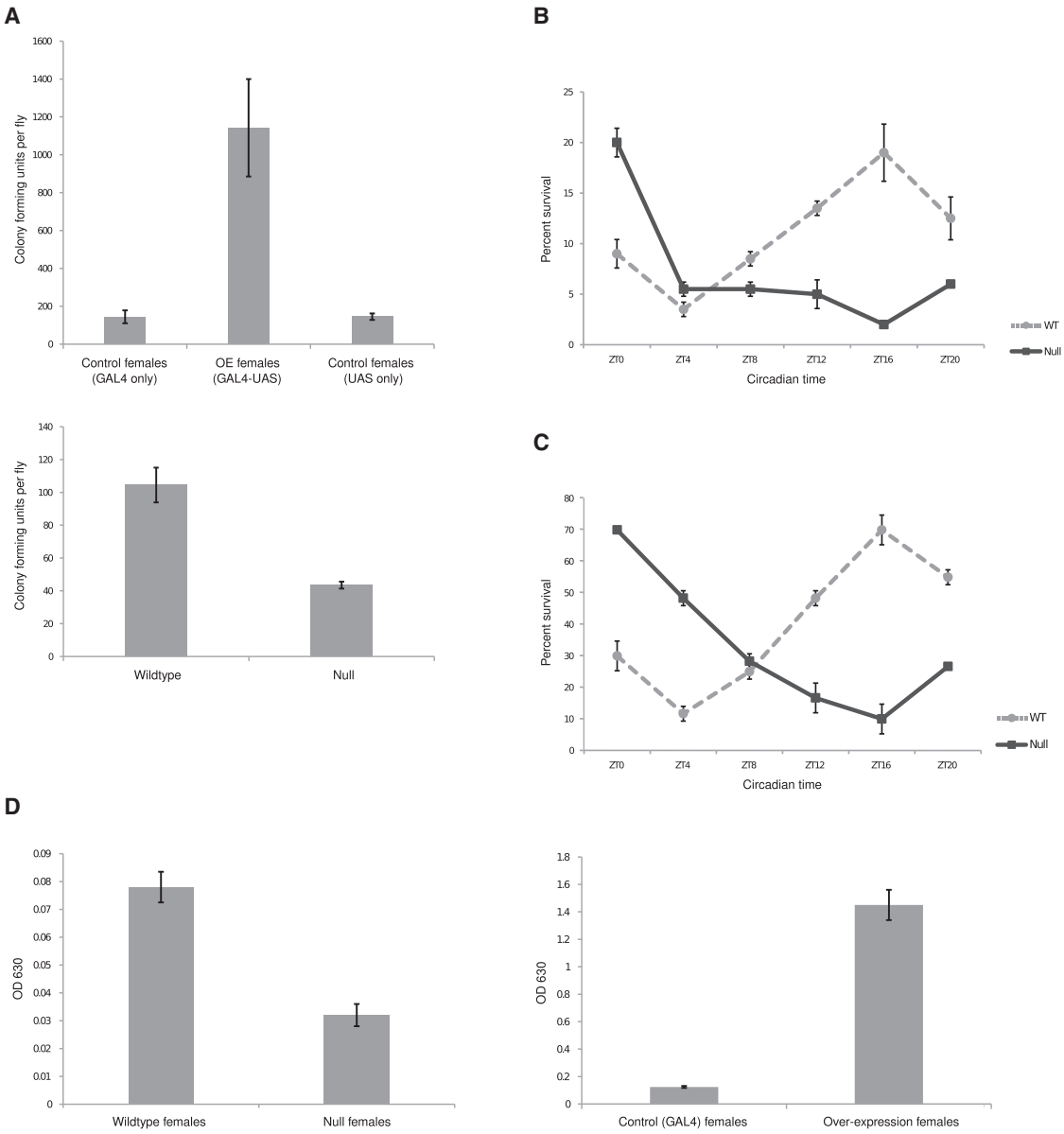

Figure 4. The Cluster miRNAs Modulate Feeding and Immunity

(A) To investigate whether miRNA cluster affects immunity, we compared immune response of WT, knockout, and miRNA overexpression flies and assayed the levels of bacteria from the peak survival time point ZT17 (Lee and Edery, 2008). Female flies were entrained under LD conditions for 3 days and used for injections on the fourth day. Twenty flies were infected with *P. aeruginosa* at the peak survival time point, ~ZT17, and fly extract was prepared after 24 hr. Serial dilutions of the extract were plated on LB plates with gentamycin, and number of colony-forming units per fly were calculated (cfu/fly). Null flies showed lower bacterial titer in response to the immune challenge in comparison to the wild-type flies. The cluster overexpression flies showed 7-fold more bacterial titers in comparison to the two control flies (*tim-gal4* and uas lines).

(B) Wild-type (*w1118*) and null flies were infected with PA14 plcs at different times of the day during LD cycles as described in Lee and Edery (2008), and percent survival was calculated using values from two different experiments. Error bars indicate standard deviation.

(C) As in (B) above, except the bacterial stock was diluted to 0.5× of what was used in (B).

(D) Flies overexpressing the cluster eat more in response to starvation, whereas the null flies eat less under the same conditions. Female flies were entrained for 3 days under LD conditions, and the feeding assay was performed on the fourth day. Null flies eat less food in response to starvation, whereas female flies overexpressing the cluster eat ~11 times more after starvation in comparison to the control strain (*tim-gal4* flies). The error bars indicate standard deviation.

i.e., ZT20 and ZT0, and fail to achieve the normal increase characteristic of ZT4, ZT8, and ZT12 (Figure 5A). Cluster pri-miRNA expression was affected similarly (Figure 5B). *Bantam* miRNA levels, assayed in parallel, were unaffected by starvation (Figure 5A), and there was little or no effect on *per* mRNA levels or cycling (Figure 5B). The observations suggest that feeding leads to transcription of the cluster and that this regulation occurs downstream of the central clock (see the Discussion). Although

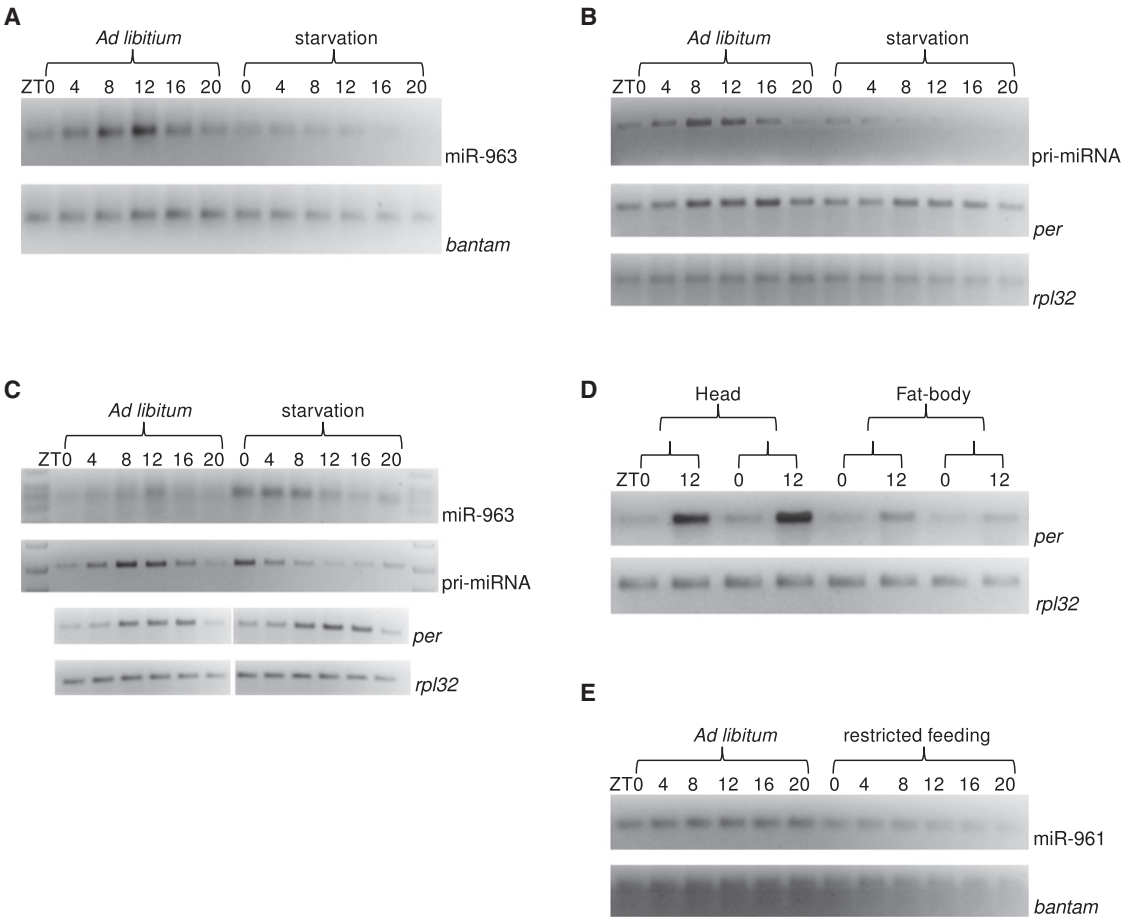

Figure 5. Transcription of the Cluster Is under Food Control

Total RNA was extracted from fly heads across six different circadian time points under ad libitum (AL) and starvation (S) conditions. *Canton S* flies were starved for at least 8 hr before lights on (starting no later than ZT16) and then collected for RNA extraction every 4 hr after that (e.g., ZT0 flies were starved for 8 hr, whereas ZT20 flies were starved for 28 hr). RNA levels were then assayed using RT-PCR and compared to the flies fed AL.

(A) The levels of mature miRNAs were assayed under AL and S conditions. The levels showed robust oscillation under AL conditions in WT but remained low under S conditions. Bantam was used as a control and did not show any significant difference under AL and S conditions.

(B) The levels of the pri-miRNA also did not show any oscillation under S conditions and remained low, indicating that food is controlling the expression of the miRNA cluster. The effect of starvation on circadian clock was assayed by measuring the levels of one of the core clock gene transcripts, *per* whose levels and cycling did not show any significant difference under AL and S conditions. *rpl32* was used as a control, and its levels were unchanged under the experimental conditions.

(C) Feeding time determines the phase of the cluster expression. Flies were subjected to a restricted feeding (RF) paradigm and fed for only 2 hr from ZT10 to ZT12. The levels of mature and pri-miRNA were assayed across circadian time. As shown earlier under AL conditions, the levels of the mature and the pri-miRNA peak at around ZT12, and this peak shifts to around ZT0-4 under RF paradigm, strongly suggesting that the peak expression is determined by the time of feeding. Circadian clock was assayed by measuring the levels of *per* mRNA, and we did not observe any significant difference under AL and RF conditions. *rpl32* was used as a control, and its levels were unchanged under the experimental conditions.

(D) Flies were entrained for 3 days under AL conditions and on the fourth day were shifted to RF paradigm as described in the Experimental Procedures. Fat -body from the abdomen was purified on the fifth day of RF paradigm and *per* mRNA levels were assayed from fat-body and fly heads. Restricted feeding had no effect on the phase and the levels of *per* mRNA. The mRNA for *rpl32* was assayed as a control.

(E) *per01* flies were subjected to the RF paradigm as described in the Experimental Procedures, and the oscillation of the cluster miRNAs was assayed using RT-PCR. The levels of the mature miRNA do not show any oscillation in *per01* flies under AL and RF conditions.

the tissue heterogeneity of *Drosophila* heads complicates this interpretation, RNA analysis after dissection of different tissues suggests that it is correct: starvation inhibited cluster miRNA expression in the brain and abdominal fat body as well as the head with little or no effect on *bantam* or *per* mRNA cycling (Figure S5).

The strong effect of starvation suggests that the phase of cluster miRNA transcription might be determined by the phase of feeding. This is because flies feed predominantly in the early morning (Seay and Thummel, 2011; Xu et al., 2008), a few hours before cluster miRNA and pri-miRNA levels begin to rise (Figures 2A, 2B, and 2D). We tested this prediction explicitly, by subjecting flies to a restricted feeding regimen. They were fed for only 2 hr, between ZT10 and ZT12, which is almost 12 hr out of phase from their normal feeding time peak of ZT0 to ZT2 under ad libitum conditions (Xu et al., 2008).

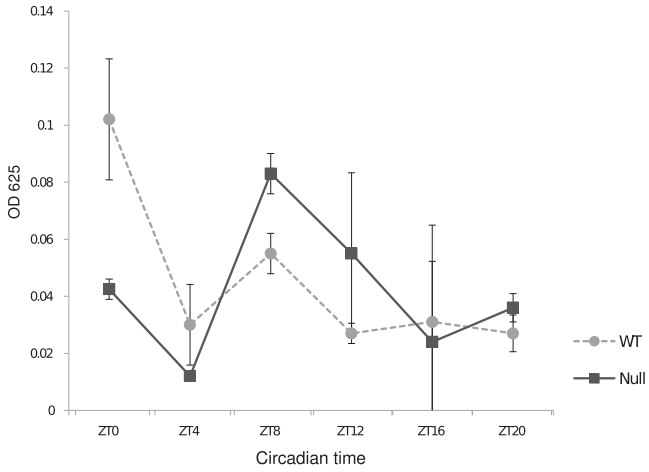

Figure 6. Cluster miRNAs Regulate Feeding Time in *Drosophila melanogaster*

Feeding rhythms of wild-type and cluster null flies under LD conditions. Following entrainment in LD conditions for 3 days, flies were fed blue dye food for 2 hr at six different time points over a 24 hr cycle. Fly bodies were separated from heads and homogenized in PBS, and the absorbance was measured at 625 nm. Flies shifted to normal food were used as controls, and their absorbance at 625 nm was subtracted from the flies that ate blue-dye food. The experiment was repeated two times, and relative food consumption was double plotted across circadian time. The error bars indicate standard deviation.

The results indeed show that the phase of cluster miRNA expression as well as pri-miRNA expression in heads is shifted by almost 12 hr under these restricted feeding conditions, with little or no effect on *per* mRNA expression (Figure 5C). There was similarly little effect of restricted feeding on *per* mRNA isolated from dissected abdominal fat body (Figure 5D), certainly nothing comparable to the dramatic effect on the phase of cluster miRNA expression. This suggests that restricted feeding impacts cluster miRNA expression downstream of the central clock. However, the clock is necessary for this effect of restricted feeding, as it cannot restore cluster miRNA cycling to the arrhythmic per^{01} strain (Figure 5E; see the Discussion).

Is this relationship between feeding time and cluster expression reciprocal, i.e., do the cluster miRNAs regulate feeding time under normal ad libitum conditions? To address this issue, we used the assay of Xu et al. (2008) to compare feeding time between the cluster KO strain and its wild-type parental strain under ad libitum conditions. The assay with the wild-type strain recapitulates published observations: there is a quite strong feeding peak at about dawn or ZT0 with a secondary peak during the late day/early night (Figure 6). The KO strain shows a reduced dawn peak and a larger secondary peak (Figure 6). This alteration in the feeding curve is very similar to that of the fully arrhythmic *clkJRK* strain (Xu et al., 2008), indicating that the cluster miRNAs make a substantial contribution to the circadian control of feeding time.

The data taken together suggest that feeding regulates the circadian cycling of the cluster miRNAs, predominantly at the transcriptional level and downstream of the core clock. The cycling miRNAs then regulate numerous physiological processes including metabolism and immune function as well as foraging and feeding time. A successful feeding event will lead to upregulation of the cluster miRNAs a few hours later, which then feeds back to downregulate metabolic and immune functions as well as foraging and feeding functions characteristic of the late night and early morning. Near the end of the night, miRNA levels fall to minimal values, which lead to an upregulation of these functions. This miRNA-mediated posttranscriptional circuit allows the fly to properly regulate the daily cycle of feeding and other physiological functions (see the Graphical Abstract).

DISCUSSION

Using Illumina deep sequencing of small RNAs from *Drosophila* heads, we identified a small set of miRNAs that undergo robust circadian cycling. We focused on six of them, which appear to be synthesized together on a single pri-miRNA and peak at the end of the day. Although the data implicate the activity of a circadian transcriptional activator or repressor in the regulation of the six cluster miRNAs, the clock probably also contributes to the short half-lives required for robust miRNA cycling. RNA profiling after manipulation of feeding indicates that the levels and cycling of the cluster miRNAs are sensitive to nutrition and/or starvation and that target functions include metabolism and innate immunity. Indeed, overexpression and especially deletion phenotypes indicate a robust miRNA effect on immunity and feeding. The data taken together suggest that the circadian clock regulates the timing of food intake, which regulates cluster miRNA cycling. These oscillations in turn regulate the daily cycling of multiple physiological processes. As feeding upregulates the cluster miRNAs with a likely downregulation of physiologically relevant mRNAs, we suggest that a successful feeding bout upregulates transcription of the cluster miRNAs to modulate mRNA translation associated with starvation, feeding, and stress. As feeding resumes when miRNA levels are low, the data suggest that the cluster miRNAs and their timing contribute to a feedback circuit that regulates daily feeding.

It may be relevant that the all six cluster miRNAs have low read numbers, explaining perhaps why they escaped detection in previous less-sensitive attempts to identify cycling miRNAs (Yang et al., 2008). There are 22 other miRNAs with similar low read numbers; most of these appear noncycling, making the relationship between the low read numbers and cycling uncertain. *Bantam* in contrast has an average read number approximately 3,500 greater than the peak values of the individual cluster miRNAs, and the previously identified cycling miRNAs, 263a and 263b (Yang et al., 2008), also have much higher read numbers than the cluster miRNAs (Figure S6). It is notable that we did not detect cycling of these two miRNAs (all time points were ±20% of each other) as compared to an amplitude of at least 5-fold for the cluster miRNAs in the same assay (Figure 1A and Figure S6).

The sequencing indicates low cluster miRNA levels around ZT0 (Figure 1A), and this conclusion is reinforced by the PCR assays (Figure 2A). Nonetheless, the miRNAs could be cyclically processed by U addition to their 3′ ends, precluding an assignment to the genome at these times (Ameres et al., 2010; Ibrahim et al., 2010; Kim et al., 2010). However, we searched the RNA sequencing data without success for partial miRNA sequences

with the addition of noncoded U residues (Ameres et al., 2010). This suggests transcriptional regulation, which is also consistent with the very similar phase and amplitude of pri-miRNA cycling.

Although the location of the primers used to assay pri-miRNA (Figure S1) suggests a single transcription unit, it is still possible that there are two primary transcripts, one of which includes miRNAs 959–962 and the other miRNAs 963–964. This would explain the presence of miRNAs 963–964 in the KO strain (Figure 3B). However, these observations can be equally well accommodated by a single transcription start site and regulatory region unaffected by the deletions. In either case, we assume that this regulatory region still functions properly despite the internal additions/deletions created by homologous recombination. It presumably controls the expression of *Gal4* in the knockin strain, which cycles robustly and similarly to cluster miRNA cycling (Figure 3C). Fat body expression is consistent with the immune and metabolism functions suggested by the mRNA analyses; the latter might include the response to noxious food components including genotoxic substances (Table 1). Feeding and immunity are also indicated by the phenotypic characterization of the KO and overexpression strains. Interestingly, it is not known whether pericerebral or abdominal fat body is more important for the expression of immunity-relevant molecules (N. Silverman, personal communication).

The peak pri-miRNA phase implicates a cycling transcriptional activator, with peak activity at about ZT12. Although this timing is compatible with a direct role for the master positive transcription factor CLK-CYC, CLK tiling and ChIP-seq data show no indication of binding to DNA within or near the cluster, which contrasts with other miRNA genes (Abruzzi et al., 2011; K. Abruzzi, personal communication). An activator downstream of the core clock is therefore indicated. Equally possible is cycling of a downstream repressor with minimal activity at about ZT12 (Sancar et al., 2011).

Both of these possibilities are compatible with the starvation response, which reinforces this transcription-centric view. The absence of cycling and low levels of the pri-miRNA as well as the cluster miRNAs (Figures 5A and 5B) indicate that starvation freezes the normally cycling activity of the key activator at a low level, or it freezes the key repressor at a high level. Restricted feeding provides a similar indication: activity of the putative activator must increase or the putative repressor decrease a few hours after feeding. Intriguingly, all of this appears to occur downstream of the core oscillator, as *per* mRNA cycling—phase as well as amplitude—is largely unaffected by starvation (Figure 5C).

These results are reminiscent of restricted feeding experiments on mammalian liver (Damiola et al., 2000; Hara et al., 2001). Importantly, they had prominent effects on the core clock within the liver. The prominent difference with mammals may reflect the strong effect of light and cryptochrome on clock gene mRNA oscillations in flies, especially in peripheral tissues (Plautz et al., 1997; Stanewsky et al., 1998); these presumably include the fat body. Consistent with our reasoning are results of a starvation experiment in which RNA from abdominal fat body was assayed. It indeed indicates that the food effects on cluster miRNA transcription occur downstream of the central clock (Figure S5). Although this conclusion differs from recent results indicating a major effect of the feeding on the fat body central clock (Xu et al., 2011), those experiments were done in constant darkness. We therefore prefer the interpretation that the central clock "wins" over food under standard light-dark entrainment conditions and that the observed feeding effects on the cluster miRNAs shown here occur downstream of the central clock. However, we cannot rule out the possibility that the pericerebral fat body, the major source of the cluster miRNAs in our experiments, is different from abdominal fat body.

The data also point to important posttranscriptional regulation of the cluster miRNAs by the clock. For example, cluster miRNA levels are not only noncycling in the arrhythmic *per01* strain background, but pri-miRNA levels are also relatively high and mature miRNA levels low. One interpretation is that Drosha processing of the cluster pri-miRNA is inefficient in *per01* flies. Given the direct role of PER in transcriptional regulation (Menet et al., 2010), cluster miRNA processing efficiency may be coupled to circadian transcription (Obernosterer et al., 2007; Thomson et al., 2006).

In a similar vein, even the short half-lives of these six miRNAs may be linked to circadian transcription. The similar pri-miRNA and miRNA circadian profiles suggest cytoplasmic miRNA half-lives of no longer than an hour or two; much longer would give rise to dampened and delayed mature miRNA profiles relative to that of pri-miRNA (Gatfield et al., 2009). Although not unprecedented (Chatterjee and Grosshans, 2009; Bail et al., 2010; Krol et al., 2010; Burns et al., 2011; Rissland et al., 2011), rapid miRNA turnover is unusual. Perhaps their common transcription is relevant to their short half-lives. In addition, a relationship of this nature might help explain the miRNA response to starvation in *per01* flies. Starvation dramatically increases mature miRNA levels in this strain without a comparable effect on pri-miRNA levels (Figure S7), suggesting that the aberrant transcriptional regulation during starvation of the *per01* strain may be unable to maintain the coupling of short miRNA half-life to transcription; stable miRNA expression may result as a default state. Consistent with coupling to transcriptional regulation, the cluster miRNAs have long half-lives when expressed in S2 cells under *actin* promoter control (data not shown).

However, we have no insight into the mechanism responsible for the normal instability of the cluster miRNAs in vivo. 3′ → 5′ exoribonucleases have been shown to play a role in miRNA degradation in plants and animals (Ramachandran and Chen, 2008), whereas the 5′ → 3′ exonuclease Xrn2 has been implicated in *C. elegans* (Chatterjee and Grosshans, 2009). Two recent studies indicate that extensive base pairing between miRNAs and their targets leads to miRNA degradation (Ameres et al., 2010; Cazalla et al., 2010). Although we do not find runs of untemplated nucleotides in our sequencing of the cluster miRNAs (data not shown), it is still possible that target mRNA cycling is necessary for the cluster miRNA short half-lives and cycling rather than vice versa.

We also have no particular insight into cluster miRNA mechanism of action. Current dogma dictates that the alterations in miRNA levels should change target mRNA translation and levels. This view is consistent with our microarray assays from the KO and overexpression strains (Table S1). Although these two strains are not complete opposites (the KO strain is missing four of the six miRNAs, whereas the overexpression strain increases levels of all six), there are many mRNAs that move in

opposite directions in the two strains: up in the deletion strain and down in the overexpression strain. Despite the likelihood of indirect effects in the two strains, some mRNAs are candidate direct targets of miRNAs 959–962, with good target sequences in their 3′UTRs. Some of these respond in traditional S2 cell reporter gene assays to cluster miRNA addition (Figure S4). Taken together with the miRNA fat body expression and the functions of metabolism and immunity as indicated by the coding sequences of putative target mRNAs (Table 1), they may contribute to the feeding- and immunity-related phenotypes affected in the deletion and the overexpression strains. However, we have not identified specific mRNA targets that contribute to these phenotypes.

These effects on innate immunity functions, feeding and foraging (Figures 4A–4D, Figure 6, and Movie S1) indicate that these cycling processes (Lee and Edery, 2008; Seay and Thummel, 2011; Wang et al., 2011; Xu et al., 2008) are influenced by these miRNAs. Given the effect of the cluster KO on ad libitum feeding (Figure 6), it is even possible that there is no direct effect of the circadian clock on the timing of feeding; all clock regulation may occur via the cluster miRNAs. As their expression is strongly regulated by feeding (Figures 5A and 5C), a feedback circuit is indicated (Graphical Abstract). Its timing must also reflect the temporal parameters that govern the synthesis and turnover of the cluster miRNAs. Although this circuit integrates circadian and environmental timing (Graphical Abstract), its mechanism is unknown. We speculate that two transcription factors function together on the promoter of the cluster miRNAs: one is a circadian factor required for transcription or perhaps even for cycling transcription, whereas the other is a nutrient-regulated factor that determines the phase of cycling. A major future challenge will be to understand the molecular mechanism that underlies this integration of circadian and environmental regulation.

EXPERIMENTAL PROCEDURES

Fly Strains

clkJRK, *tim-GAL4* (yw;*tim-GAL4*/CyO), and *clkAR* flies were described previously (Allada et al., 1998, 2003; Kaneko and Hall, 2000). The plasmid pUAST-CLU was generated by cloning a 2.4 kb genomic DNA fragment, 500 bases upstream and downstream of the Dme-miR-959 and Dme-miR-964, respectively, into the XhoI and XbaI sites of pUAST vector. The cloning was confirmed by restriction digestion and conventional sequencing. The transgenic yw;UAS-CLU/CyO fly line was generated by The Best Gene (http://thebestgene.com/). The transgenic fly line was then crossed to *tim-GAL4*/CyO to generate *timgal4,* UAS-CLU stable lines. The miR-959-962 KO mutant was generated using homologous recombination based ends-out gene targeting (Gong and Golic, 2003). Upstream and downstream homology arms flanking miR-959-962 cluster were amplified and cloned into the targeting vector *pW25-Gal4-attB2* (Weng et al., 2009) using primer pairs 5′-GCGGCCGCCGC TCGACTATTCTGCACTT and 5′-GCGGCCGCTTAATTAATGCACTGCTTTAG CATCCAC for upstream homology arm, and 5′-GGCCGGCCTCGTTGGACCA GACAATACACT and 5′-GGCCGGCCGGCCAGACAAAAA form downstream homology arm. Donor transgene was obtained by integrating targeting vector into landing strain, *ZH-attP-86Fb* (Bischof et al., 2007) as described in Chen et al. (2011). The targeting vector *pW25-Gal4-attB2* would allow *Gal4* knockin at targeted locus; therefore *miR-959-962 cluster-Gal4 KO* is a *Gal4* knockin mutant and can be used as a *Gal4* driver to report the cluster expression pattern. *miR-959-962 cluster KO^{w-}* was generated from *Gal4* knockin mutant by using *Cre/loxP* recombination to excise both *Gal4* and *mini-white* genes (Weng et al., 2009).

RNA Extraction and RT-PCR

Total RNA from fly heads was extracted using TRIzol reagent (Invitrogen) as suggested by the supplier. For RT-PCR analysis, 5 μg of total RNA was treated with RQ1 DNase (Promega) as described by the supplier. From this, 2 μg was used for reverse transcription reaction using Superscript II and random hexamers. Where required, transcript-specific reverse transcription was performed using a gene-specific primer. Cycling parameters for the PCR reaction were 94°C for 2 min followed by 28 cycles of 94°C for 30 s, 55°C for 45 s, and 72°C for 1 min. miRNA RT-PCR was essentially performed as described by Chen et al. (2005). RP49 and Bantam were used as controls for mRNA and miRNA RT-PCRs, respectively. Primers used for various gene-expression analyses are described in Table S2.

Preparation of Small RNA Sequencing Libraries

Small RNA sequencing libraries were essentially prepared as described in Seitz et al. (2008), with one exception. The 2S rRNA was depleted by hybridizing to a DNA oligonucleotide followed by RNaseH treatment. Following depletion of 2S rRNA, 19–29 nucleotide long RNAs were gel purified, and adapters were ligated at 3′ and 5′ end using Rnl2([1–249], Ho et al., 2004) and T4 RNA ligase (Ambion), respectively. RNA was PCR amplified using primers corresponding to the adapters, and the PCR products were gel purified on a 2% agarose gel. The libraries were sequenced using the Illumina deep sequencing platform. Reads were aligned to the genome with Seqmap (Jiang and Wong, 2008) using the first 20 bases and allowing at most one mismatch. Mature miRNA sequences downloaded from miRBase were then aligned to this subset of reads. Only mature sequences completely contained within the read with at most two mismatches were kept. The miRNA reads were then normalized to total reads.

Microarrays and Expression Analysis

Total RNA was extracted as described above, and the probes for the arrays were prepared as described by the supplier (Affymetrix). Hybridization of the probes, staining, and washing were done according to the manufacturer's protocol. The normalized $\log_2$ values were obtained from CEL files using the GCRMA algorithm in the Bioconductor analysis package for the R software.

Feeding Assays

The feeding assay was as described in Xu et al. (2008). Briefly, 2- to 5-day-old female flies were entrained at 25°C in LD under ad libitum (AL) conditions for 3 days. On the fourth day in LD, flies were shifted from normal food to either blue-color food (15% sucrose/1% agar diets containing 1% FD&C Blue number 1 McCormick) or non-dye-containing food for 2 hr. The flies were homogenized in PBS and centrifuged at 14,000 rpm for 30 min. The absorbance of the supernatant was measured at 625 nm. The flies shifted to no-dye-containing food served as controls, and their absorbance was subtracted from the supernatant of the flies fed with food containing blue dye. Feeding assays in response to starvation were done by starving the flies for 24 hr. Female flies were entrained for 3 days in LD cycle under ad libitum conditions and were shifted to starvation vials at ZT0 on the fourth day. Following 24 hr starvation, flies were shifted to either blue-color food (as above) or non-dye-containing food for 15 min. Samples were processed as above, and the absorbance was measured at 625 nm.

Pseudomonas aeruginosa Infections and Survival Rates

PA14 plcs strain of *P. aeruginosa* was a kind gift from Laurence Rahme. *P. aeruginosa* was cultured as described in Lee and Edery (2008). Female flies were entrained for 3 days in LD and infected on the fourth day. Flies were anesthetized using CO_2, and a 10 μm tungsten needle (Ted Pella, Inc.) was used for pricking. Tungsten needle was dipped into the concentrated bacterial culture and pricked gently on the surface of the abdomen to prevent injury to the internal organs. Following infections, flies were returned to the same LD conditions, and their survival was counted 48 hr postinfection.

Bacterial Growth Assay

Twenty-four hours following infections, flies were rinsed once with 70% ethanol to eliminate bacteria from the surface. Fly extract was prepared by homogenizing flies in ice-cold LB media, and serial dilutions were plated on LB agar plates containing gentamycin. The plates were incubated at 37°C

overnight, and visible colonies on the plates were counted manually. Colony-forming units per fly were averaged (Cfu/fly) and plotted for comparison.

S2 Cell Transfection Assays

S2 cells were cultured in insect tissue culture media (HyClone) containing 10% FBS (GIBCO). Cells were seeded in a 6-well plate, and transfections were performed at ~80% confluence using Cellfectin (Invitrogen) as suggested by the supplier. Of luciferase reporter constructs, 50 ng were cotransfected with 50 ng of either the wild-type or mutated seed sequence pAc-CLU plasmid. Forty-eight hours posttransfection, luciferase assays were performed using the Dual-Luciferase Reporter Assay system (Promega).

Statistical Analysis

Data from two independent experiments were averaged and plotted in Microsoft Excel. Statistical significance was calculated using standard deviation.

ACCESSION NUMBERS

Sequencing and microarray data are deposited on the Gene Expression Omnibus (GEO) database under the accession number GSE40981 (GEO, http://www.ncbi.nlm.nih.gov/geo/query/acc.cgi?acc=GSE40981).

SUPPLEMENTAL INFORMATION

Supplemental Information includes seven figures, one movie, two tables, Supplemental Experimental Procedures, and Supplemental References and can be found with this article online at http://dx.doi.org/10.1016/j.cmet.2012.10.002.

ACKNOWLEDGMENTS

We thank C. Li and P. Zamore for the small RNA cloning protocol, and L. Rahme for the PA14 *plcs* strain and the fly injection protocol. We thank P. Chilakamarri for help with fly dissections. We are also grateful to S. Kadener, P. Nawathean, M. Marr, N. Lau, and members of the Rosbash laboratory for critical comments and suggestions. This work was supported in part by NIH grants GM023549 and NS045713 to M.R.

Received: March 6, 2012
Revised: June 7, 2012
Accepted: October 8, 2012
Published online: November 1, 2012

REFERENCES

Abruzzi, K.C., Rodriguez, J., Menet, J.S., Desrochers, J., Zadina, A., Luo, W., Tkachev, S., and Rosbash, M. (2011). Drosophila CLOCK target gene characterization: implications for circadian tissue-specific gene expression. Genes Dev. *25*, 2374–2386.

Allada, R., and Chung, B.Y. (2010). Circadian organization of behavior and physiology in Drosophila. Annu. Rev. Physiol. *72*, 605–624.

Allada, R., White, N.E., So, W.V., Hall, J.C., and Rosbash, M. (1998). A mutant Drosophila homolog of mammalian Clock disrupts circadian rhythms and transcription of period and timeless. Cell *93*, 791–804.

Allada, R., Kadener, S., Nandakumar, N., and Rosbash, M. (2003). A recessive mutant of Drosophila Clock reveals a role in circadian rhythm amplitude. EMBO J. *22*, 3367–3375.

Alvarez-Saavedra, M., Antoun, G., Yanagiya, A., Oliva-Hernandez, R., Cornejo-Palma, D., Perez-Iratxeta, C., Sonenberg, N., and Cheng, H.Y. (2011). miRNA-132 orchestrates chromatin remodeling and translational control of the circadian clock. Hum. Mol. Genet. *20*, 731–751.

Ameres, S.L., Horwich, M.D., Hung, J.H., Xu, J., Ghildiyal, M., Weng, Z., and Zamore, P.D. (2010). Target RNA-directed trimming and tailing of small silencing RNAs. Science *328*, 1534–1539.

Bail, S., Swerdel, M., Liu, H., Jiao, X., Goff, L.A., Hart, R.P., and Kiledjian, M. (2010). Differential regulation of microRNA stability. RNA *16*, 1032–1039.

Bischof, J., Maeda, R.K., Hediger, M., Karch, F., and Basler, K. (2007). An optimized transgenesis system for Drosophila using germ-line-specific phiC31 integrases. Proc. Natl. Acad. Sci. USA *104*, 3312–3317.

Burns, D.M., D'Ambrogio, A., Nottrott, S., and Richter, J.D. (2011). CPEB and two poly(A) polymerases control miR-122 stability and p53 mRNA translation. Nature *473*, 105–108.

Cazalla, D., Yario, T., and Steitz, J.A. (2010). Down-regulation of a host microRNA by a Herpesvirus saimiri noncoding RNA. Science *328*, 1563–1566.

Chatterjee, S., and Grosshans, H. (2009). Active turnover modulates mature microRNA activity in Caenorhabditis elegans. Nature *461*, 546–549.

Chen, C., Ridzon, D.A., Broomer, A.J., Zhou, Z., Lee, D.H., Nguyen, J.T., Barbisin, M., Xu, N.L., Mahuvakar, V.R., Andersen, M.R., et al. (2005). Real-time quantification of microRNAs by stem-loop RT-PCR. Nucleic Acids Res. *33*, e179. http://dx.doi.org/10.1093/nar/gni178.

Chen, Y.W., Weng, R., and Cohen, S.M. (2011). Ptrotocols for use of homologous recombination gene targeting to produce microRNA mutants in Drosophila. Methods Mol. Biol. *732*, 99–120.

Cheng, H.Y., Papp, J.W., Varlamova, O., Dziema, H., Russell, B., Curfman, J.P., Nakazawa, T., Shimizu, K., Okamura, H., Impey, S., and Obrietan, K. (2007). microRNA modulation of circadian-clock period and entrainment. Neuron *54*, 813–829.

Damiola, F., Le Minh, N., Preitner, N., Kornmann, B., Fleury-Olela, F., and Schibler, U. (2000). Restricted feeding uncouples circadian oscillators in peripheral tissues from the central pacemaker in the suprachiasmatic nucleus. Genes Dev. *14*, 2950–2961.

Gatfield, D., Le Martelot, G., Vejnar, C.E., Gerlach, D., Schaad, O., Fleury-Olela, F., Ruskeepää, A.L., Oresic, M., Esau, C.C., Zdobnov, E.M., and Schibler, U. (2009). Integration of microRNA miR-122 in hepatic circadian gene expression. Genes Dev. *23*, 1313–1326.

Ghildiyal, M., and Zamore, P.D. (2009). Small silencing RNAs: an expanding universe. Nat. Rev. Genet. *10*, 94–108.

Golombek, D.A., and Rosenstein, R.E. (2010). Physiology of circadian entrainment. Physiol. Rev. *90*, 1063–1102.

Gong, W.J., and Golic, K.G. (2003). Ends-out, or replacement, gene targeting in Drosophila. Proc. Natl. Acad. Sci. USA *100*, 2556–2561.

Guo, H., Ingolia, N.T., Weissman, J.S., and Bartel, D.P. (2010). Mammalian microRNAs predominantly act to decrease target mRNA levels. Nature *466*, 835–840.

Hara, R., Wan, K., Wakamatsu, H., Aida, R., Moriya, T., Akiyama, M., and Shibata, S. (2001). Restricted feeding entrains liver clock without participation of the suprachiasmatic nucleus. Genes Cells *6*, 269–278.

Ho, C.K., Wang, L.K., Lima, C.D., and Shuman, S. (2004). Structure and mechanism of RNA ligase. Structure *12*, 327–339.

Ibrahim, F., Rymarquis, L.A., Kim, E.J., Becker, J., Balassa, E., Green, P.J., and Cerutti, H. (2010). Uridylation of mature miRNAs and siRNAs by the MUT68 nucleotidyltransferase promotes their degradation in Chlamydomonas. Proc. Natl. Acad. Sci. USA *107*, 3906–3911.

Jiang, H., and Wong, W.H. (2008). SeqMap: mapping massive amount of oligonucleotides to the genome. Bioinformatics *24*, 2395–2396.

Kadener, S., Menet, J.S., Sugino, K., Horwich, M.D., Weissbein, U., Nawathean, P., Vagin, V.V., Zamore, P.D., Nelson, S.B., and Rosbash, M. (2009). A role for microRNAs in the Drosophila circadian clock. Genes Dev. *23*, 2179–2191.

Kaneko, M., and Hall, J.C. (2000). Neuroanatomy of cells expressing clock genes in Drosophila: transgenic manipulation of the period and timeless genes to mark the perikarya of circadian pacemaker neurons and their projections. J. Comp. Neurol. *422*, 66–94.

Karginov, F.V., Cheloufi, S., Chong, M.M., Stark, A., Smith, A.D., and Hannon, G.J. (2010). Diverse endonucleolytic cleavage sites in the mammalian transcriptome depend upon microRNAs, Drosha, and additional nucleases. Mol. Cell *38*, 781–788.

Kim, Y.K., Heo, I., and Kim, V.N. (2010). Modifications of small RNAs and their associated proteins. Cell *143*, 703–709.

Kojima, S., Gatfield, D., Esau, C.C., and Green, C.B. (2010). MicroRNA-122 modulates the rhythmic expression profile of the circadian deadenylase Nocturnin in mouse liver. PLoS ONE *5*, e11264. http://dx.doi.org/10.1371/journal.pone.0011264.

Krol, J., Busskamp, V., Markiewicz, I., Stadler, M.B., Ribi, S., Richter, J., Duebel, J., Bicker, S., Fehling, H.J., Schübeler, D., et al. (2010). Characterizing light-regulated retinal microRNAs reveals rapid turnover as a common property of neuronal microRNAs. Cell *141*, 618–631.

Kula-Eversole, E., Nagoshi, E., Shang, Y., Rodriguez, J., Allada, R., and Rosbash, M. (2010). Surprising gene expression patterns within and between PDF-containing circadian neurons in Drosophila. Proc. Natl. Acad. Sci. USA *107*, 13497–13502.

Lee, J.E., and Edery, I. (2008). Circadian regulation in the ability of Drosophila to combat pathogenic infections. Curr. Biol. *18*, 195–199.

Lim, L.P., Lau, N.C., Garrett-Engele, P., Grimson, A., Schelter, J.M., Castle, J., Bartel, D.P., Linsley, P.S., and Johnson, J.M. (2005). Microarray analysis shows that some microRNAs downregulate large numbers of target mRNAs. Nature *433*, 769–773.

Menet, J.S., Abruzzi, K.C., Desrochers, J., Rodriguez, J., and Rosbash, M. (2010). Dynamic PER repression mechanisms in the Drosophila circadian clock: from on-DNA to off-DNA. Genes Dev. *24*, 358–367.

Miyoshi, K., Miyoshi, T., and Siomi, H. (2010). Many ways to generate microRNA-like small RNAs: non-canonical pathways for microRNA production. Mol. Genet. Genomics *284*, 95–103.

Nagoshi, E., Sugino, K., Kula, E., Okazaki, E., Tachibana, T., Nelson, S., and Rosbash, M. (2010). Dissecting differential gene expression within the circadian neuronal circuit of Drosophila. Nat. Neurosci. *13*, 60–68.

Obernosterer, G., Martinez, J., and Alenius, M. (2007). Locked nucleic acid-based in situ detection of microRNAs in mouse tissue sections. Nat. Protoc. *2*, 1508–1514.

Plautz, J.D., Kaneko, M., Hall, J.C., and Kay, S.A. (1997). Independent photoreceptive circadian clocks throughout *Drosophila*. Science *278*, 1632–1635.

Ramachandran, V., and Chen, X. (2008). Degradation of microRNAs by a family of exoribonucleases in Arabidopsis. Science *321*, 1490–1492.

Rissland, O.S., Hong, S.J., and Bartel, D.P. (2011). MicroRNA destabilization enables dynamic regulation of the miR-16 family in response to cell-cycle changes. Mol. Cell *43*, 993–1004.

Sancar, G., Sancar, C., Brügger, B., Ha, N., Sachsenheimer, T., Gin, E., Wdowik, S., Lohmann, I., Wieland, F., Höfer, T., et al. (2011). A global circadian repressor controls antiphasic expression of metabolic genes in Neurospora. Mol. Cell *44*, 687–697.

Seay, D.J., and Thummel, C.S. (2011). The circadian clock, light, and cryptochrome regulate feeding and metabolism in Drosophila. J. Biol. Rhythms *26*, 497–506.

Seitz, H., Ghildiyal, M., and Zamore, P.D. (2008). Argonaute loading improves the 5′ precision of both MicroRNAs and their miRNA* strands in flies. Curr. Biol. *18*, 147–151.

Shi, L., Ko, M.L., and Ko, G.Y. (2009). Rhythmic expression of microRNA-26a regulates the L-type voltage-gated calcium channel alpha1C subunit in chicken cone photoreceptors. J. Biol. Chem. *284*, 25791–25803.

So, W.V., and Rosbash, M. (1997). Post-transcriptional regulation contributes to *Drosophila* clock gene mRNA cycling. EMBO J. *16*, 7146–7155.

Stanewsky, R., Kaneko, M., Emery, P., Beretta, B., Wager-Smith, K., Kay, S.A., Rosbash, M., and Hall, J.C. (1998). The cryb mutation identifies cryptochrome as a circadian photoreceptor in Drosophila. Cell *95*, 681–692.

Thomson, J.M., Newman, M., Parker, J.S., Morin-Kensicki, E.M., Wright, T., and Hammond, S.M. (2006). Extensive post-transcriptional regulation of microRNAs and its implications for cancer. Genes Dev. *20*, 2202–2207.

Wang, W., Barnaby, J.Y., Tada, Y., Li, H., Tör, M., Caldelari, D., Lee, D.U., Fu, X.D., and Dong, X. (2011). Timing of plant immune responses by a central circadian regulator. Nature *470*, 110–114.

Weng, R., Chen, Y.W., Bushati, N., Cliffe, A., and Cohen, S.M. (2009). Recombinase-mediated cassette exchange provides a versatile platform for gene targeting: knockout of miR-31b. Genetics *183*, 399–402.

Woo, K.C., Kim, T.D., Lee, K.H., Kim, D.Y., Kim, W., Lee, K.Y., and Kim, K.T. (2009). Mouse period 2 mRNA circadian oscillation is modulated by PTB-mediated rhythmic mRNA degradation. Nucleic Acids Res. *37*, 26–37.

Woo, K.C., Ha, D.C., Lee, K.H., Kim, D.Y., Kim, T.D., and Kim, K.T. (2010). Circadian amplitude of cryptochrome 1 is modulated by mRNA stability regulation via cytoplasmic hnRNP D oscillation. Mol. Cell. Biol. *30*, 197–205.

Xu, K., Zheng, X., and Sehgal, A. (2008). Regulation of feeding and metabolism by neuronal and peripheral clocks in Drosophila. Cell Metab. *8*, 289–300.

Xu, K., DiAngelo, J.R., Hughes, M.E., Hogenesch, J.B., and Sehgal, A. (2011). The circadian clock interacts with metabolic physiology to influence reproductive fitness. Cell Metab. *13*, 639–654.

Yang, M., Lee, J.E., Padgett, R.W., and Edery, I. (2008). Circadian regulation of a limited set of conserved microRNAs in Drosophila. BMC Genomics *9*, 83. http://dx.doi.org/10/1186/1471-2164-9-83.